frontiers | Frontiers in Earth Science

TYPE Original Research
PUBLISHED 17 February 2025
DOI 10.3389/feart.2025.1476135

OPEN ACCESS

EDITED BY
Carmen Sanchez-Valle,
University of Münster, Germany

REVIEWED BY
Zhenlong Song,
Southern University of Science and Technology, China
Xinyu Liang,
Shanxi University, China

*CORRESPONDENCE
Shaowei Zhang,
zhangshaowei@xatu.edu.cn

RECEIVED 05 August 2024
ACCEPTED 27 January 2025
PUBLISHED 17 February 2025

CITATION
Zhang S, Dang F and Guan H (2025) The thixotropic mechanical properties and microscopic mechanism of lime-modified loess.
Front. Earth Sci. 13:1476135.
doi: 10.3389/feart.2025.1476135

The thixotropic mechanical properties and microscopic mechanism of lime-modified loess

Shaowei Zhang[1,2]*, Faning Dang[2] and Hao Guan[1]

[1]School of Civil and Architecture Engineering, Xi'an Technological University, Xi'an, China, [2]School of Civil Engineering and Architecture, Xi'an University of Technology, Xi'an, China

The thixotropy of lime-modified loess is a key engineering problem in large-scale mountain levelling and urban construction on the Loess Plateau in China. We analyse the thixotropic factors and establish thixotropic models of modified loess at macroscales and microscales to interpret the evolution of the thixotropic mechanism of lime-modified loess. A custom-made volume-preserving thixotropic instrument is used to eliminate the influence of consolidation deformation on thixotropy and simulate soil consolidation in the field. Consolidated undrained triaxial tests, nuclear magnetic resonance analysis, and electron microscopy are used to investigate the thixotropy of soils with different thixotropic periods (0 days, 7 days, 14 days, 21 days, 42 days, 84 days, 126 days, and 168 days). The results show that the failure strength increases and the growth rate decreases with the thixotropic period length. The failure strength increases rapidly in the early thixotropic stage; the inflexion point occurs at 21 days, and stabilisation is observed at about 42 days. The internal friction angle and cohesive force increase over time, the cohesive force increased more obviously, which was 2.94 times of the initial thixotropic period, the increase in internal friction angle is within 4°. The pore distribution is more uniform at the microscopic level, and large and small pores are transformed into medium pores over time. As the thixotropic period increases, the amount of cementitious material generated in the modified loess and the cementation degree increase, and the number of surface pits and large pores on the particles substantially decreases, resulting in numerous flower-shaped and grid structures. The thixotropic mechanism of modified loess consists of pore homogenisation, gravitational repulsion between particles, and cementation caused by the lime reaction.

KEYWORDS

microscopic structural evolution, loess, thixotropy of soil, thixotropic mechanism, thixotropic parameter

1 Introduction

Due to insufficient space for urban development, Loess Plateau cities have proposed vertical rather than horizontal expansion to develop new districts and relocate the old city and other programmes. Extensive excavation, soil removal of soil, and

the filling of ditches have been performed (Juang et al., 2019). Large-scale high-fill projects have caused the destruction of loess areas. Stabilisation of soil with lime is an economical and effective soil improvement method (Gu and Chen, 2020; Metelková et al., 2012). This method is widely used on the Loess Plateau in large-scale high-fill improvement projects to eliminate large pores and vertical fissures and improve the strength and stability of loess. The engineering performance of lime-modified loess is higher than that of natural loess. Filling gullies disrupts the long-term geological equilibrium, and it requires a long time for the lime-modified fill to achieve sufficient bearing capacity. Thus, the foundation soil experiences uneven stress under external loads (Park et al., 2015; Jeong et al., 2015), resulting in differential settlement and causing foundation failures and building collapses (Hu et al., 2017; Abu-Farsakh et al., 2015).

The thixotropy of loess (Li et al., 2020) refers to a significant reduction in soil strength due to a disturbance. The soil regains its strength after the cessation of the disturbance, resulting in a new equilibrium system between the soil particles, cations, and water molecules after a rest period (Zhang et al., 2013; Yang and Andersen, 2016; Rinaldi and Clariá, 2016). Zhang et al. (2017) investigated the thixotropic behaviour of Zhanjiang clay in southern China using scanning electron microscopy (SEM) and mercury intrusion porosimetry. They found that changes in the internal force field of the soil cause a transition from a dispersed to a flocculation state. Thixotropy is an adaptive adjustment of the structure. Tang et al. (2022a); Tang et al. (2021); Tang et al. (2022b) assessed the thixotropy of structural clay in the Zhanjiang Formation of the Beibu Gulf region and investigated the effects of the disturbance degree, physical and mechanical soil properties, overlying pressure, and the presence of water on the thixotropy of the Zhanjiang Formation clay. Ren et al. (2024); Yang et al. (2021); Wang et al. (2023) researched the effects of thixotropy and consolidation on an increase in the undrained shear strength of deep-sea soil. They assessed the influence and mechanism of reconsolidation on the thixotropy of soft deep-sea soil and determined the long-term trend of soil strength. Shahriar et al. (2018) observed that the maximum strength recovery of samples occurred at a water content of 0.75 times the w_L. Seng and Tanaka (2012) found a significant thixotropic effect on the shear modulus at a water content close to the w_L. More detailed information on the thixotropic parameters and mechanical characteristics of loess has been described by Wei et al. (2023a); Wei et al. (2023b).

Research on loess has focused on its strength, deformation, wetting, freezing, thawing, and dynamic properties (Xu et al., 2022; Hu et al., 2022; Zhou et al., 2020; Zhou et al., 2018; Li et al., 2016). However, few studies have investigated the thixotropic properties of loess. The soil volume is fixed during thixotropy in many tests. Thus, eliminating the effect of a strength increase on thixotropy due to soil consolidation is challenging. The measured strength includes the strength due to soil consolidation and the thixotropic strength, and it is impossible to differentiate between the compression consolidation and the thixotropic properties. In addition, the mechanism of thixotropy of loess is unknown, and the fine structural evolution, the relationship between the soil particle activities and the pore water, and the link between fine structural changes and macroscopic strength are unclear (Peng et al., 2021; Peng et al., 2024; Wang et al., 2022; Ren et al., 2021; Tan et al., 2024; Xue et al., 2024). We used a custom-made volume-preserving thixotropy apparatus to create samples, eliminate the effect of a change in the consolidation volume on thixotropy, and improve the sample homogeneity. Consolidated undrained triaxial tests, nuclear magnetic resonance (NMR) tests, and electron microscopy are conducted to examine the thixotropic properties of soils in different thixotropic periods (0 days, 7 days, 14 days, 21 days, 42 days, 84 days, 126 days, 168 days). The evolution of the pore structure is analysed at the macroscale and microscale to interpret the thixotropic mechanism of lime-modified loess.

2 Materials and methods

2.1 Materials and sample preparation

The soil for the test was obtained from a steep bank in Xi'an City, Shaanxi Province, at a depth of 7.0–8.0 m. The soil was immediately placed in a black soil bag that was sealed to prevent moisture loss and labelled with the depth, time and vertical orientation. The samples were placed on shock-absorbing cushioning material in the vehicle and transported back to the indoor laboratory. The soil samples were cubes with a side length of 35 cm, consisting of uniformly hard, yellowish-brown Q_3 loess. The soil extraction site is shown in Figure 1.

The bags were inspected for damage before unsealing them to ensure that they were not torn. The soil samples were removed, crushed, and passed through a 2 mm geotechnical sieve. The water content, specific gravity, liquid-plastic limit, and other basic physical property indices of the soil samples were determined according to the Chinese Standard for Geotechnical Test Methods (GB/T 50123-2019). The results are listed in Table 1.

2.2 Test methods

2.2.1 Volume-preserving thixotropic apparatus and sampling methods

A custom-made thixotropic apparatus (Figure 2) was used to create samples similar to the compression process of modified loess in the engineering. This device simulates the consolidation of loess after resting and maintains the soil volume constant during the thixotropic period. It eliminates the influence of consolidation factors and ensures that the soil strength can be attributed to the thixotropic characteristics rather than the soil consolidation. This method allows for distinguishing between compression consolidation and the thixotropic properties of the soil. The equipment consists of a steel plate, I-beam, jack, screw, steel cylinder, and other components. The soil samples were placed into the lower steel plate model box. The jack provided a counterforce and compressed the soil body using a fixed displacement and fixed bolts during the thixotropic period (0 days, 7 days, 14 days, 21 days, 42 days, 84 days, 126 days, and 168 days). The volume remained the same during this period. At the end of the thixotropic period, the steel plate was removed, and the soil was moved away from the side wall using a sample chipper. Standard triaxial samples with a dimension of 3.91 cm × 8 cm were created.

FIGURE 1
Soil extraction site.

TABLE 1 Basic physical property indices of the loess specimens.

Natural water content ω/%	Density ρ(g/cm^3)	Liquid limit ω_L/%	Plastic limit ω_p/%	Plasticity index I_p	Optimal moisture content ω_{op}/%	Maximum dry density ρ_{dmax}
18.10	1.63	31.95	20.82	11.13	16.86	1.62

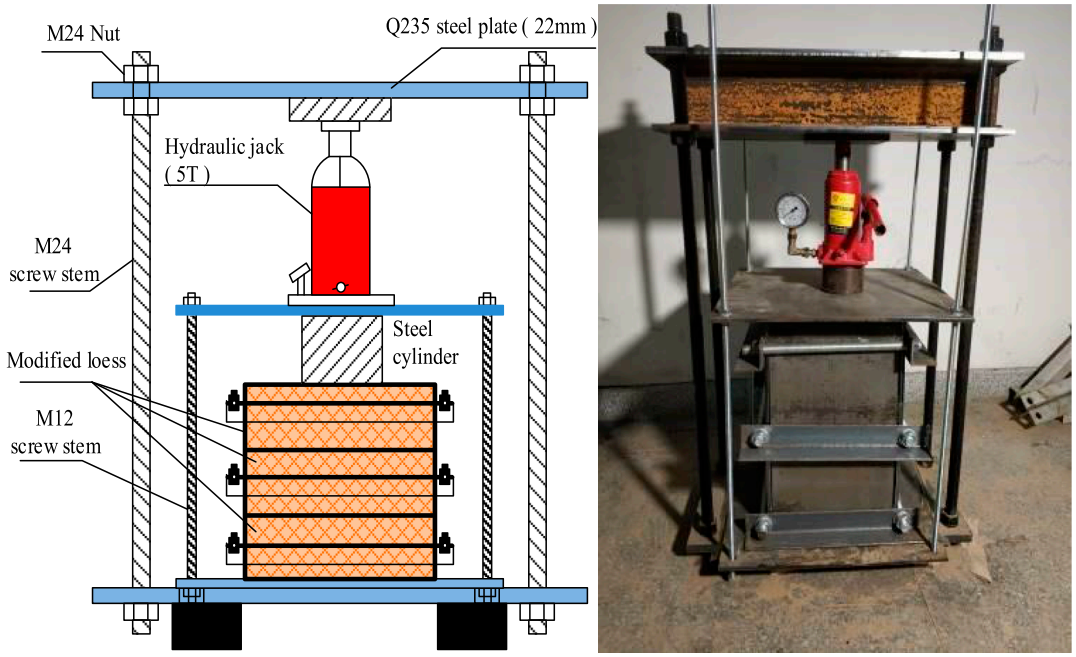

FIGURE 2
Structure of the custom-made thixotropic apparatus.

2.2.2 Macro mechanical property tests

The GDS triaxial test system was used to conduct consolidated undrained triaxial tests under different peripheral pressures (50 kPa, 100 kPa, 200 kPa) on eight modified soil samples in the thixotropic stage. The samples had 17% water content, 1.5 g cm^{-3} dry density, and contained 3%, 6%, and 9% of a lime admixture. The test was terminated when the axial strain reached 15%. The peak load, breaking strength, cohesive force, and angle of internal friction were recorded.

2.2.3 Nuclear magnetic resonance test to assess fine-scale pore changes

The principle of nuclear magnetic resonance (NMR) is to obtain the distribution spectrum of longitudinal signal strength

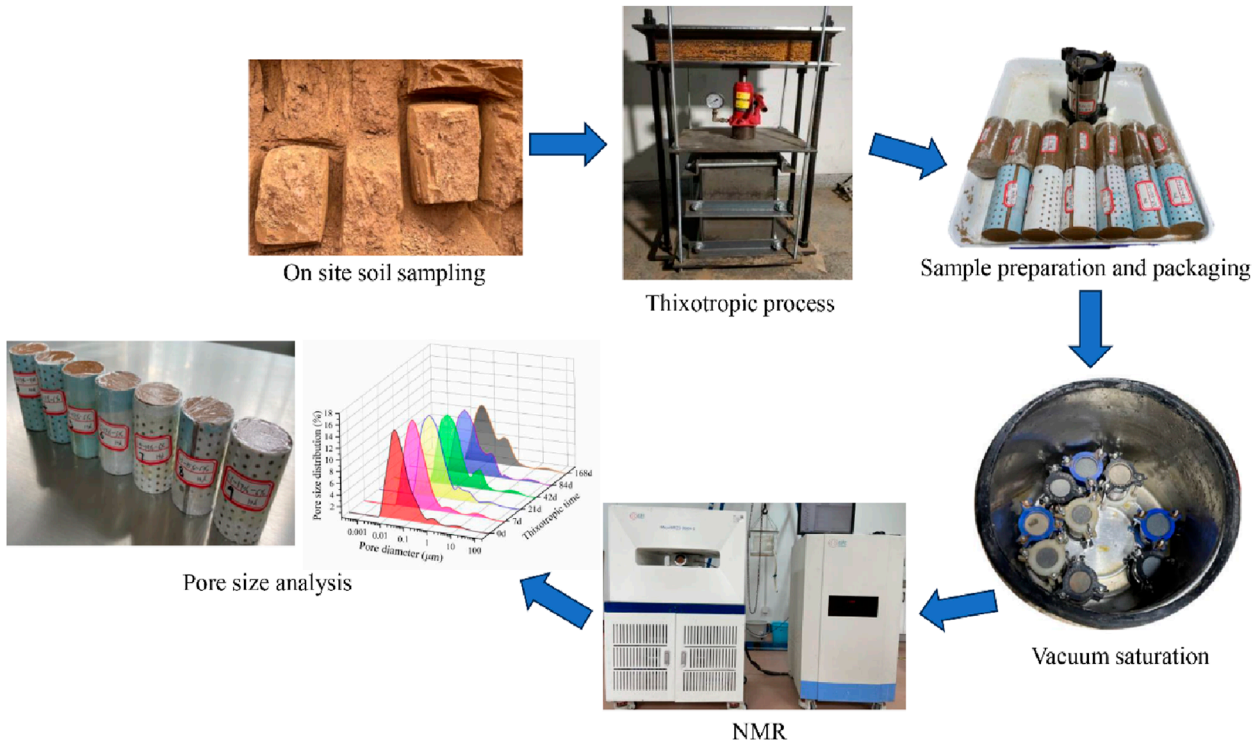

FIGURE 3
The fine-scale pore analysis steps.

and transverse relaxation time T_2 by measuring the relaxation characteristics of hydrogen ions in soil pore water. Derivation of T_2 and Pore Radius Relationship as follows:

$$\frac{1}{T_2} \approx \rho_2 \frac{2}{R}$$

Where ρ_2 represents the surface relaxation strength, which is dependent on the material properties, R is the pore radius. The smaller the T_2 value, the smaller the pore radius R; The larger the T_2 value, the larger the pore radius R.

Fine-scale pore changes in the lime-modified loess due to thixotropy were assessed using MesoMR23-060H-I NMR tests. The change in the pore number during the thixotropic period was examined for different pore sizes to determine fine-scale structural changes. The modified loess specimens for six thixotropic periods were vacuum-saturated and subjected to NMR tests. The T_2 distribution was analysed. The modified loess samples had a water content of 17%, a dry density of 1.5 g cm^{-3}, and a lime proportion of 6%. The thixotropic periods were 0 days, 7 days, 21 days, 42 days, 84 days, and 168 days. The analysis steps are shown in Figure 3.

2.2.4 Evolution of microscopic particles of lime-modified loess

Changes in the microscopic particle structure of lime-modified loess due to the thixotropic effects were assessed using SEM (Phenom-World Phenom XL) at 1000x magnification. We determined the degree of internal cementation and the filling degree of the particles and pore spaces with the newly generated gelatinous material. The water content of modified loess was 17%, the dry density was 1.5 g cm^{-3}, the lime proportion was 6%, and the thixotropic periods were 0 days, 7 days, 21 days, 42 days, 84 days, and 168 days. The analysis steps are shown in Figure 4.

3 Results

3.1 Thixotropic mechanical properties of lime-modified loess

3.1.1 Strength recovery characteristics

Figure 5 shows the relationship between the shear strength of modified loess and the thixotropic period for different lime contents and consolidation pressures. The strength increases, and the growth rate decreases as the thixotropy period increases for all lime contents and pressures. The strength increases faster in the early thixotropy period, and an inflexion point occurs at 21 d subsequently, the curve stabilises at about 42 days.

We use the peripheral pressure of 100 kPa as an example. The strength increases from 1014.80 kPa to 2212.62 kPa as the thixotropic period increases from 0 days to 168 days for a lime content of 3%, an increase of 218%. For a 6% lime content, the breaking strength increases from 1101.57 kPa to 2486.15 kPa, an increase of 226%. For a 9% lime content, the breaking strength increases from 1374.58 kPa to 2652.13 kPa, an increase of 193%.

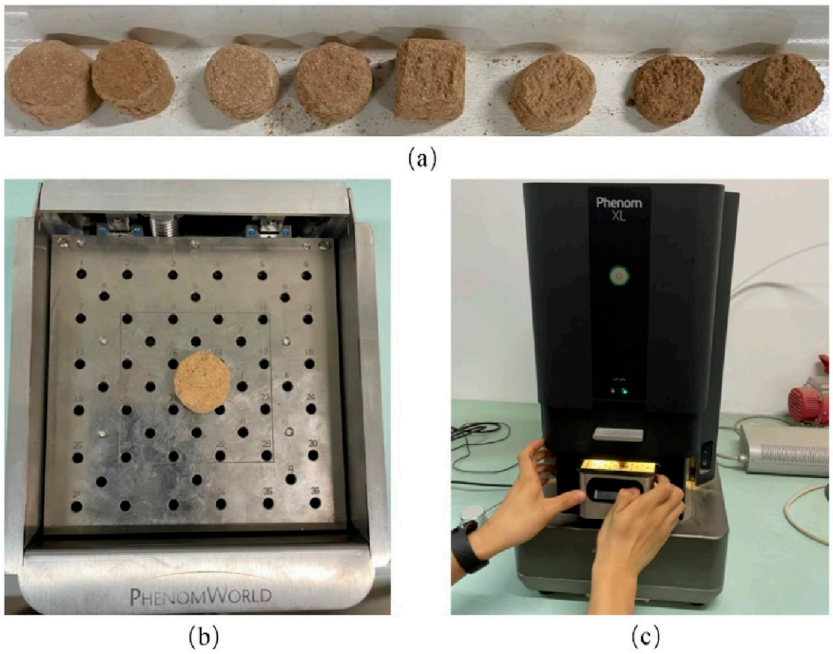

FIGURE 4
Sample preparation **(A)**, installation **(B)** and microstructure analysis **(C)**.

3.1.2 Cohesion and internal friction angle characteristics

The Mohr's circle strength envelope was plotted according to the peak bias stresses of the three lime-modified loess samples at different confining pressures. The relationship between the cohesion c, the angle of internal friction φ, and the thixotropic period is shown in Figure 6. The internal friction angle and cohesion increase with the thixotropic period. The curve flattens after 21 days. The rate of increase is higher for the cohesion than for the internal friction angle. The increase in cohesion from 0 days to 168 days is 294%, 227%, and 201% for lime contents of 3%, 6%, and 9%, respectively. In contrast, the internal friction angle only increases by 4°.

3.1.3 Thixotropic parameter of lime-modified loess based on triaxial shear strength

The thixotropic parameter reflects the thixotropic properties of the soil. We used the shear strength index c and φ derived from the triaxial test to establish a thixotropic parameter of the lime-modified loess based on the triaxial shear strength J_t. J_t is the ratio of the shear strength of the lime-modified loess at a given time in the thixotropic period to the shear strength in the thixotropic period 0 days.

The thixotropic parameter of the lime-modified loess at rest t is defined as:

$$J_t = \frac{\tau_{f.t}}{\tau_{f.0}} = \frac{c_t + \left[\frac{1}{2}(\sigma_1+\sigma_3) - \frac{1}{2}(\sigma_1-\sigma_3)\sin\varphi_t\right]\tan\varphi_t}{c_0 + \left[\frac{1}{2}(\sigma_1+\sigma_3) - \frac{1}{2}(\sigma_1-\sigma_3)\sin\varphi_0\right]\tan\varphi_0}$$

where c_t, φ_t、 and $\tau_{f.t}$ denote the cohesion, friction angle, and ultimate shear strength, respectively, obtained from the triaxial shear test after the compression of the lime-modified loess in the thixotropic period t; c_0、 φ_0、 and $\tau_{f.0}$ denote the cohesion, friction angle, and ultimate shear strength, respectively, obtained from the triaxial shear test after the compression of the lime-modified loess in the thixotropic period 0 days.

Figure 7 shows the relationship between the thixotropic parameters of the three lime-modified loess samples and the thixotropic period under a confining pressure of 100 kPa. The larger the thixotropic parameter J_t, the higher the degree of thixotropy of the soil. The J_t values of the samples with lime contents of 3%, 6%, and 9% increase. The value is the largest for the sample with 6% lime content. This curve stabilises first (21 days), and the curves for the samples with 3% and 9% lime content stabilise at about 42 days. The thixotropic parameter values of the modified loess with different lime contents are 2.11, 2.23, and 1.88, respectively, at 168 days.

3.2 Pore size distribution in different thixotropic periods

NMR tests were conducted to determine the relationship between the pore relaxation time T_2 and the signal intensity for the lime-modified loess samples in different thixotropic periods. The transverse relaxation time T_2 is directly proportional to the pore radius R. The pores were categorised into small (d < 0.4 μm), medium (0.4 μm ≤ d < 4.0 μm), and large pores (d ≥ 4.0 μm).

Figure 8 shows the pore size distribution in different thixotropic periods for the sample with a 6% lime content. The curves have three peaks and show that small pores have the highest proportion. As the thixotropic period increases from 0 days to 168 days, the peak intensity decreases, and the peak shifts from 0.02 μm to 0.06 μm. The proportion of small pores is 15.2% at 0 days and 9.7% at 168 days. A smaller peak is observed for the mesopores. The proportion of pores in the range of 0.4 μm–4.0 μm pores increases with the thixotropic period from 0

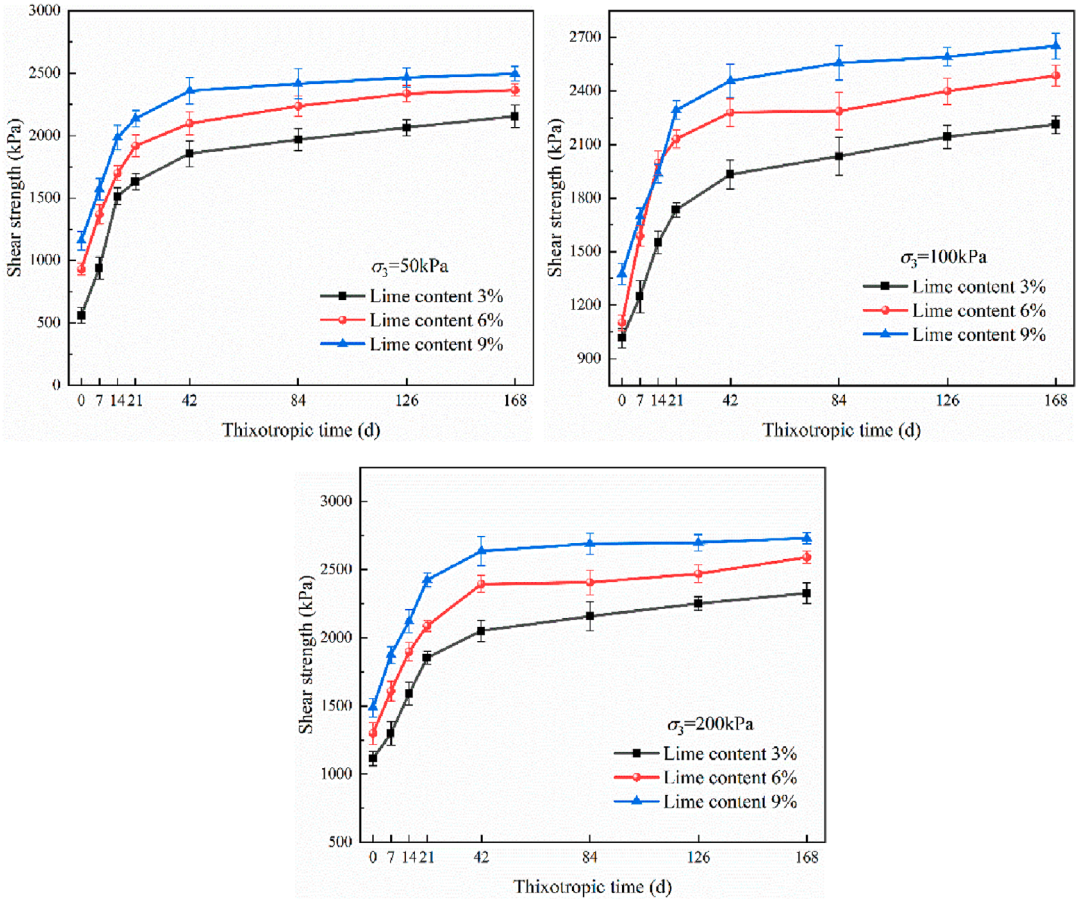

FIGURE 5
Relationship between the shear strength of modified loess and the thixotropic times for different lime contents and consolidation pressures.

days to 168 days. The proportion of mesopores is 1.1% at 0 days, 3.3% at 42 days, and 4.7% at 168 days. The proportion of macropores is the smallest. It increases negligibly from 0 days to 168 days.

Figure 9 shows the pore size distribution of samples with different lime contents for the thixotropic period of 7 days. Small pores have the largest proportion, followed by medium and large pores. As the lime content increases from 3% to 9%, the proportion of small pores increases from 11.2% to 17.7%. The proportion of mesopores decreases as the lime content increases from 3% to 6% and then remains stable. The change in the macropores is not significant.

3.3 Micromorphology changes during the thixotropic period

The SEM images of the lime-modified loess in six thixotropic periods (0 days, 7 days, 21 days, 42 days, 84 days, and 168 days) are shown in Figure 10.

Large pores and pits between the particles are observed at 0 days and 7 days. The aggregates are loose and scattered, with a few rods and fibrous structures. Some colloidal compounds occur, and the degree of interparticle cementation and stability are low. At 21 days and 42 days, the number of large pits, pores, and aggregates on the specimen surface has increased, and the degree of cementation has increased significantly. Many flower-like structures and grids occur on the surface of the aggregates and soil particles. This is the crystalline lattice of quicklime, hydrated calcium silicate, and calcium aluminates resulting from the crystallisation of volcanic ash in the limestone loess. The number of pits and large pores on the surface is much lower at 84 days and 168 days, consistent with the NMR test results. The large intergranular voids have been filled by particles, and the surface of the soil particles and aggregates is covered by lamellar and flocculent structures. The soil samples are dense and exhibit good properties. In addition, the cementitious materials harden as the thixotropic period increases, forming a protective film on the soil particles and cementing the particles together. As a result, the density and integrity of the soil samples are improved, increasing the strength of the modified loess.

4 Discussion of mechanisms

In this section, the experimental results of the present study and previous findings (Zhang et al., 2017; Ren et al., 2021) are utilized to comprehensively and systematically discuss the thixotropic mechanism of lime-modified loess from the microcosmic point

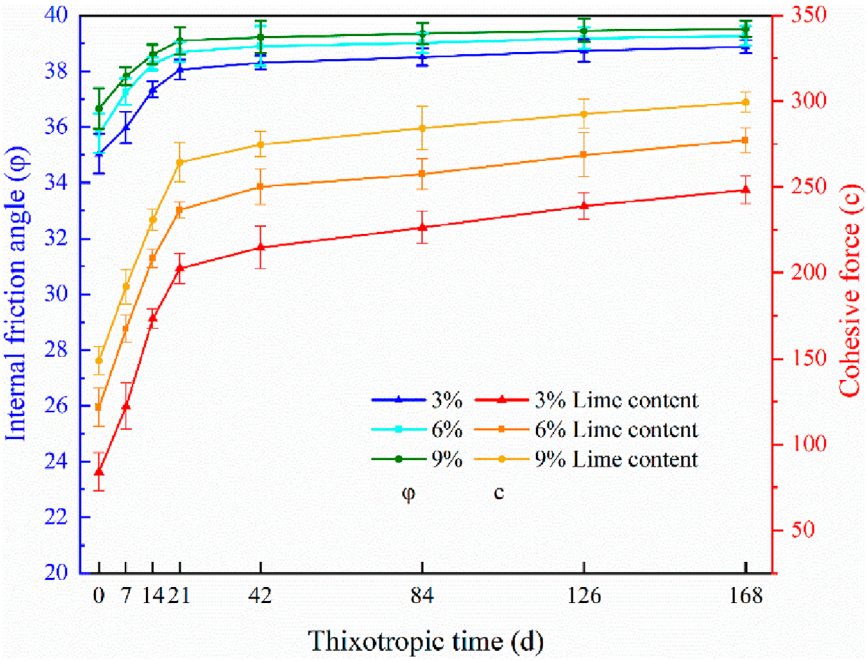

FIGURE 6
Relationship between internal friction angle, cohesive force, and thixotropic period for different lime dosages.

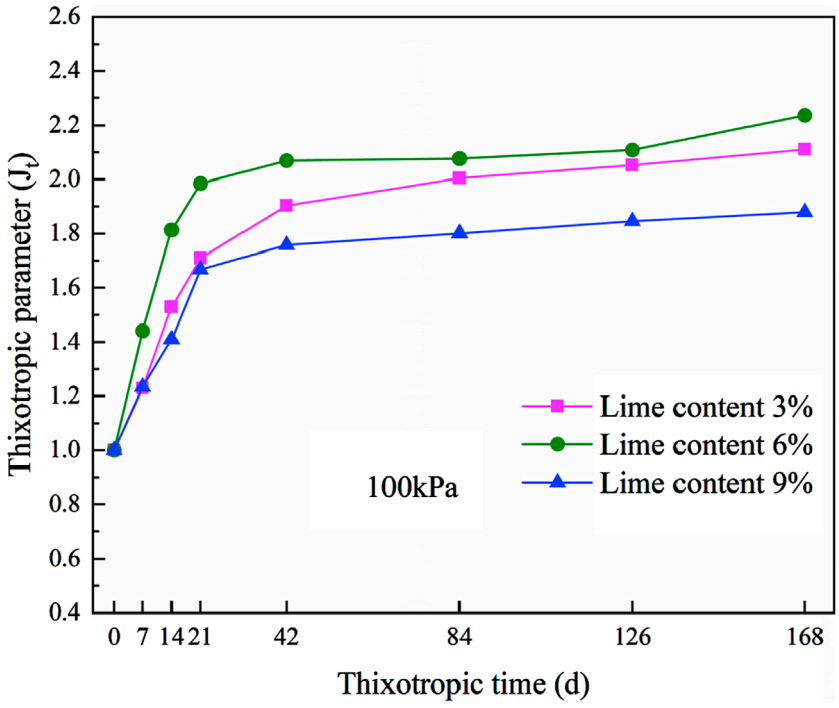

FIGURE 7
Relationship between the thixotropic parameter and the thixotropic period for different lime dosages.

of view. As the fine-scale pore size distribution changes from 0 days to 168 days, the number of small and large pores decreases, with the former decreasing more than the latter. The number of medium pores increases, indicated by an increase in the peak of the pore size distribution curve. The small pores decreased by 5.5% and the medium pores increased by 3.6% with the increase of

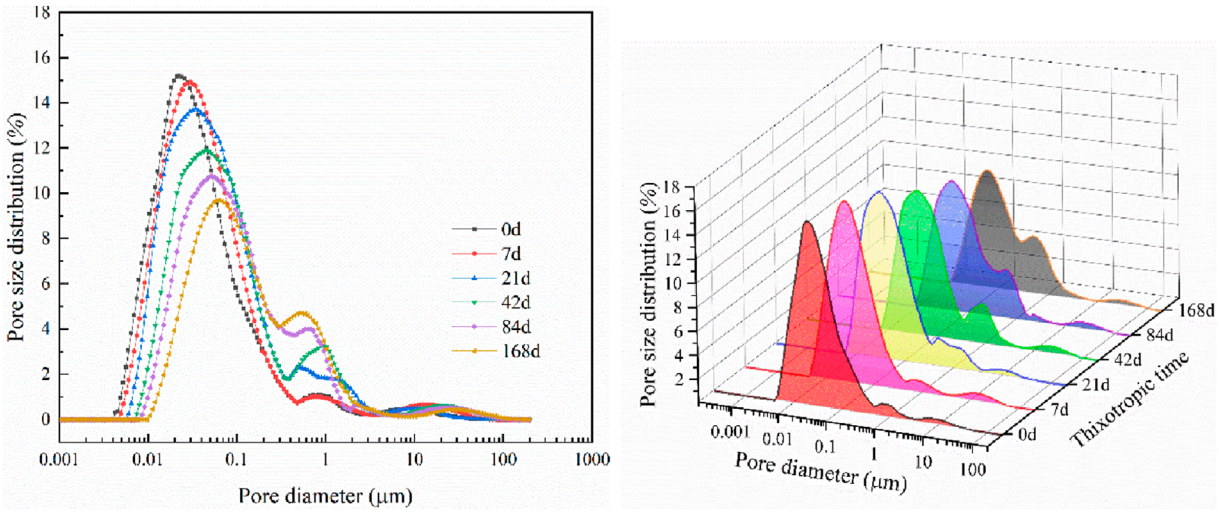

FIGURE 8
Pore size distribution in different thixotropic periods for the sample with a 6% lime content.

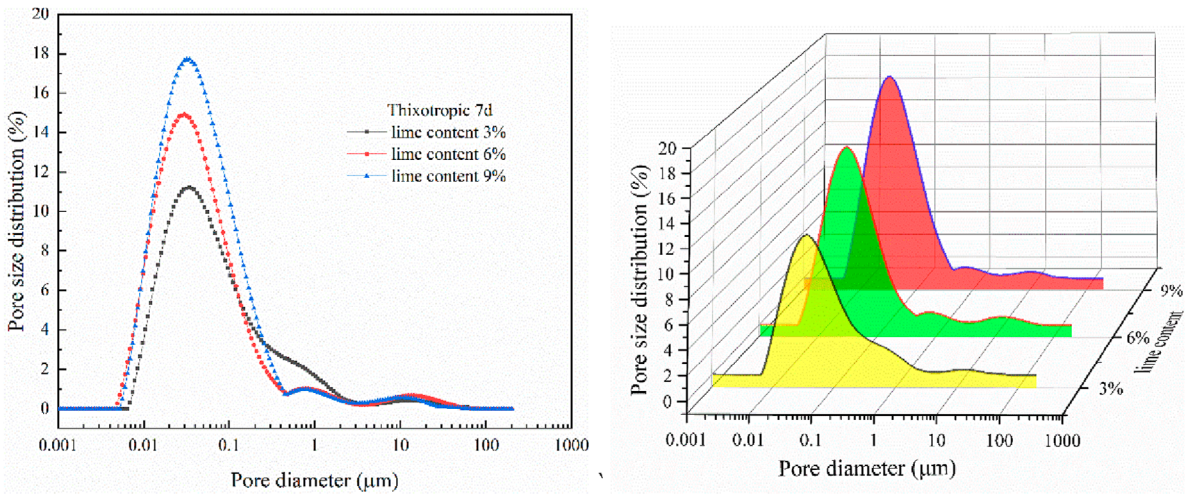

FIGURE 9
Pore size distribution of samples with different lime contents in the 7 days thixotropic period.

thixotropy (Figure 8). This finding suggests a change from small to medium pores during the thixotropic period, this is consistent with the study of Zhanjiang clay (Zhang et al., 2017). The large and small pores are transformed into medium pores, and the pore size distribution is homogenised due to a change in the soil structure attributed to the thixotropic process. The results obtained by Zhang et al. (2017) show that the particle movement results from the unbalance between attractive and repulsive forces. According to Figure 10, as the thixotropic period increases, the soil particles are displaced and coalesce, large aggregates are formed, the degree of orientation of the particles increases, and the interparticle linkage increases. Wei et al. (2023a); Wei et al. (2023b) thought that in a soil-water-electrolyte system, undisturbed loess is stable due to the balance of the particles' gravitational and repulsive forces. The interparticle linkage is destroyed after disturbance, and particles are dispersed. When the disturbance stops, the bilayer ions are redistributed, the microstructure is reorganised, the repulsive force between the particles decreases, and the gravitational force increases. Flocculation occurs when the particles are close to each other, and the structure changes from dispersed to a flocculated state after the disturbance.

Previous studies endeavored to determine the basic characteristics of Xi'an loess (Wei et al., 2023a; Wei et al., 2023b) that affect the thixotropic behavior, the chemical reaction is not the principal factor. In this work, aggregates and soil particles appear on the surface of particles during the thixotropic process. Many flower-like structures and networks are formed at 7 days–84 days, these flower-like structures in the red frame (Figure 10) represent the hydrated lime crystal grid, hydrated calcium silicate, calcium aluminate, and other cementitious substances that have been formed

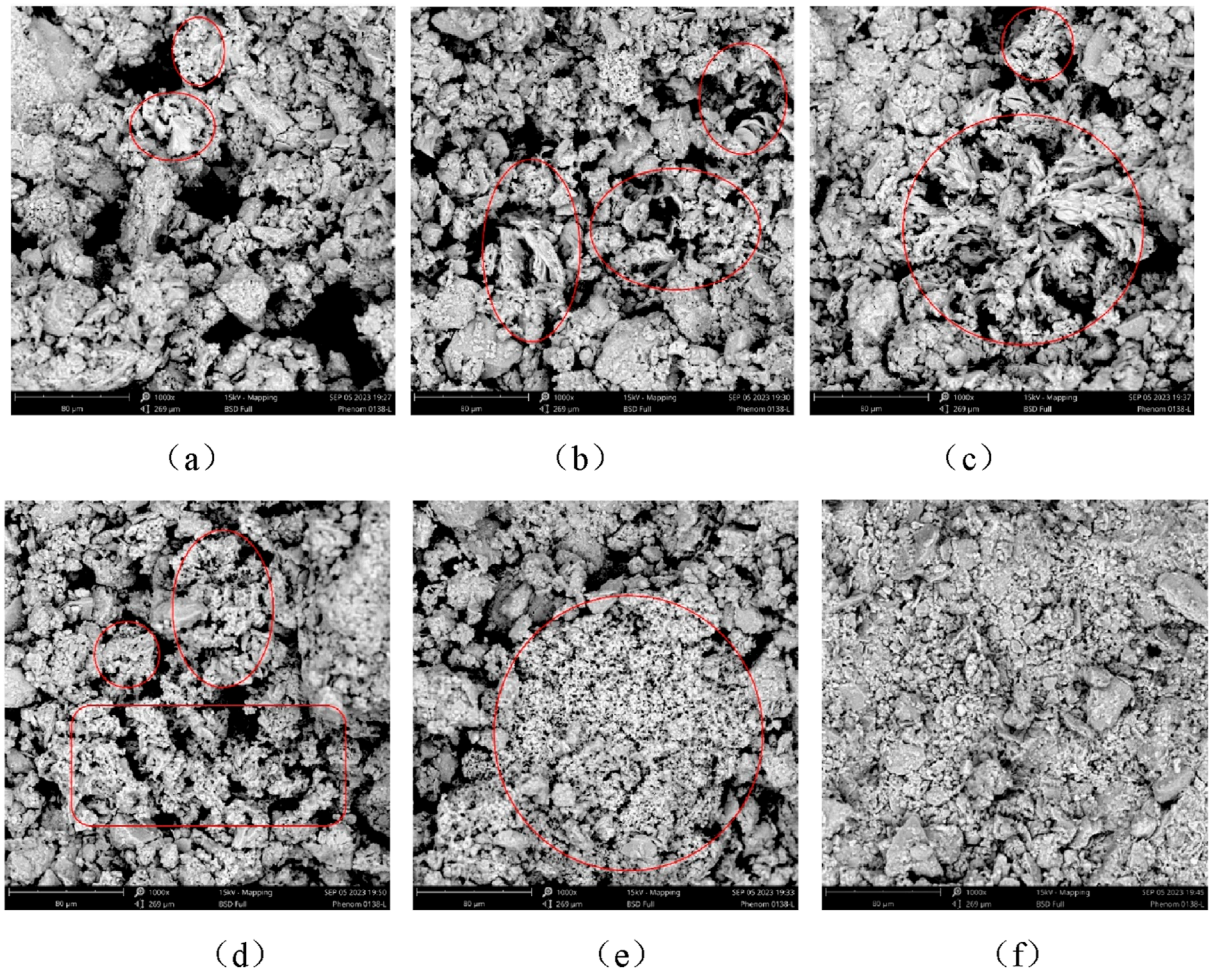

FIGURE 10
SEM images of lime-modified loess in different thixotropic periods. **(A)** 0 days **(B)** 7 days **(C)** 21 d **(D)** 42 days **(E)** 84 days **(F)** 168 days.

through crystallization and volcanic ash processes in the lime loess. In summary, according to the NMR and SEM results, the thixotropic mechanism of lime-modified loess consists of three parts: pore homogenisation, gravitational repulsion between particles, and lime-induced gelling, these three parts change the microstructure and cause flocculation. Loss of strength occurs after soil disturbance. The strength recovery due to thixotropy after resting is characterised by destruction of the soil structure, particle dispersion, and a change in the gravitational and repulsive forces between the particles, resulting in flocculation. The changes at the micro-level may be a timedependent process because of the adaptive adjustment of the structure and may result in the energy transformation process known as thixotropy.

5 Conclusion

In this study, the evolution of the strength and the microstructure of lime-modified loess during 168 days of thixotropy was evaluated to elucidate thixotropic mechanisms. The following conclusions can be drawn:

(1) The strength of the loess samples with three lime contents under different confining pressures increased as the thixotropic period increased, but the growth rate decreased. The strength increased faster in the early thixotropy period, and an inflexion point occurred at 21 days. Subsequently, the curve stabilized at about 42 days. The strength in the late thixotropic period increased at a lower rate and was 2.26 times higher than in the early thixotropic period. The angle of internal friction and the cohesion increased during the thixotropic period. The rate of increase was larger for the cohesion. It was 2.94 higher in the late thixotropic period than in the early one. In contrast, the rate of increase in the internal friction was only 4°. The maximum value of the thixotropic parameter was observed for the sample with a 6% lime content.

(2) As the thixotropic period increased from 0 days to 168 days, the peaks of small and large pores in the pore size distribution curves shifted toward the mesopores. The number of small and large pores decreased, and the rate of decrease was higher for the former than the latter. The number of mesopores increased. The structure of the lime-modified loess changed due to thixotropy. The large and small pores transformed

into medium pores, and the pore distribution became more homogeneous.

(3) The SEM images showed that the amount of cementitious materials, such as the crystalline lattice of the slaked lime, hydrated calcium silicate, and calcium aluminate, increased during the thixotropic period. The degree of cementation increased, and the number of pits and large pores on the particle surface decreased. Many floral and reticulated structures appeared, and the density and integrity of the soil samples increased. The thixotropy mechanism of the lime-modified loess consisted of a change in the microstructure and increased flocculation.

Data availability statement

The original contributions presented in the study are included in the article/supplementary material, further inquiries can be directed to the corresponding author.

Author contributions

SZ: Writing–original draft, Writing–review and editing. FD: Writing–review and editing. HG: Writing–review and editing.

Funding

The author(s) declare that financial support was received for the research, authorship, and/or publication of this article. This research is financially supported by the National Natural Science Foundation of China (NSFC) (Grant No. 51979225) and the Natural Science Foundation of Shaanxi Province, China (Grant Nos 2024JC-YBQN-0605 and 2024SF-YBXM-618).

Conflict of interest

The authors declare that the research was conducted in the absence of any commercial or financial relationships that could be construed as a potential conflict of interest.

Publisher's note

All claims expressed in this article are solely those of the authors and do not necessarily represent those of their affiliated organizations, or those of the publisher, the editors and the reviewers. Any product that may be evaluated in this article, or claim that may be made by its manufacturer, is not guaranteed or endorsed by the publisher.

References

Abu-Farsakh, M., Rosti, F., and Souri, A. (2015). Evaluating pile installation and subsequent thixotropic and consolidation effects on setup by numerical simulation for full-scale pile load tests. *Can. Geotechnical J.* 52, 1734–1746. doi:10.1139/cgj-2014-0470

Gu, K., and Chen, B. (2020). Loess stabilization using cement, waste phosphogypsum, fly ash and quicklime for self-compacting rammed earth construction. *Constr. Build. Mater* 231, 117195. doi:10.1016/j.conbuildmat.2019.117195

Hu, W., Cheng, W.-C., Wang, L., and Xue, Z.-F. (2022). Micro-structural characteristics deterioration of intact loess under acid and saline solutions and resultant macro-mechanical properties. *Soil Tillage Res.* 220, 105382. doi:10.1016/j.still.2022.105382

Hu, W., Xu, Q., Wang, G., Scaringi, G., Mcsaveney, M., and Hicher, P. (2017). Shear resistance variations in experimentally sheared mudstone granules: a possible shear-thinning and thixotropic mechanism. *Geophys Res. Lett.* 44. doi:10.1002/2017gl075261

Jeong, S. W., Locat, J., Torrance, J. K., and Leroueil, S. (2015). Thixotropic and anti-thixotropic behaviors of fine-grained soils in various flocculated systems. *Eng. Geol.* 196, 119–125. doi:10.1016/j.enggeo.2015.07.014

Juang, C. H., Dijkstra, T., Wasowski, J., and Meng, X. (2019). Loess geohazards research in China: advances and challenges for mega engineering projects. *Eng. Geol.* 251, 1–10. doi:10.1016/j.enggeo.2019.01.019

Li, P., Vanapalli, S., and Li, T. (2016). Review of collapse triggering mechanism of collapsible soils due to wetting. *J. Rock Mech. Geotechnical Eng.* 8, 256–274. doi:10.1016/j.jrmge.2015.12.002

Li, Y., Shi, W., Aydin, A., Beroya-Eitner, M. A., and Gao, G. (2020). Loess genesis and worldwide distribution. *Earth-Science Rev.* 201, 102947. doi:10.1016/j.earscirev.2019.102947

Metelková, Z., Boháč, J., Přikryl, R., and Sedlářová, I. (2012). Maturation of loess treated with variable lime admixture: pore space textural evolution and related phase changes. *Appl. Clay Sci.* 61, 37–43. doi:10.1016/j.clay.2012.03.008

Park, D., Kutter, B. L., and DeJong, J. T. (2015). Effects of thixotropy and cement content on the sensitivity of soft remolded clay. *J. Geotechnical Geoenvironmental Eng.* 141. doi:10.1061/(asce)gt.1943-5606.0001221

Peng, J., Luo, S., Wang, D., Ren, Y., Fan, L., DeGroot, D. J., et al. (2021). Quantitative evaluation of thixotropy-governed microfabric evolution in soft clays. *Appl. Clay Sci.* 210, 106157. doi:10.1016/j.clay.2021.106157

Peng, T., Fu, S., Huang, L., Chen, Z., and Cao, J. (2024). Effects of orthogonal cleat structures on hydraulic fracture evolution behavior. *Geoenergy Sci. Eng.* 241, 213119. doi:10.1016/j.geoen.2024.213119

Ren, Y., Yang, S., Andersen, K. H., Yang, Q., and Wang, Y. (2021). Thixotropy of soft clay: a review. *Eng. Geol.* 287, 106097. doi:10.1016/j.enggeo.2021.106097

Ren, Y., Zhang, S., Wang, Y., Yang, Q., and Zhou, Z. (2024). Experimental study on the thixotropic mechanism of deep-sea clay from the perspective of microstructure and bound water. *Acta Geotech.* 19, 685–698. doi:10.1007/s11440-023-01967-5

Rinaldi, V. A., and Clariá, J. J. (2016). Time dependent stress–strain behavior of bentonite slurries; effect of thixotropy. *Powder Technol.* 291, 311–321. doi:10.1016/j.powtec.2015.12.036

Seng, S., and Tanaka, H. (2012). Properties of very soft clays: a study of thixotropic hardening and behavior under low consolidation pressure. *Soils Found.* 52, 335–345. doi:10.1016/j.sandf.2012.02.010

Shahriar, A. R., Abedin, M. Z., and Jadid, R. (2018). Thixotropic aging and its effect on 1-D compression behavior of soft reconstituted clays. *Appl. Clay Sci.* 153, 217–227. doi:10.1016/j.clay.2017.12.029

Tan, P., Chen, Z., Huang, L., Zhao, Q., and Shao, S. R. (2024). Evaluation of the combined influence of geological layer property and *in-situ* stresses on fracture height growth for layered formations. *Petroleum Sci.* 21, 3222–3236. doi:10.1016/j.petsci.2024.07.014

Tang, B., Liu, T., and Zhou, B. (2022b). Duncan–chang E-υ model considering the thixotropy of clay in the Zhanjiang Formation. *Sustainability* 14, 12258. doi:10.3390/su141912258

Tang, B., Xie, L., Wang, W., Zhou, B., and Gong, Y. (2022a). Unconfined compressive strength and pore structure evolution law of structural clay after disturbance. *Front. Earth Sci.* 10. doi:10.3389/feart.2022.932621

Tang, B., Zhou, B., Xie, L., and Yin, J. (2021). Evaluation method for thixotropy of clay subjected to unconfined compressive test. *Front. Earth Sci.* 9. doi:10.3389/feart.2021.683454

Wang, N., Ren, Y., Yang, G., Sun, A., and Yang, Q. (2022). Experimental investigation on the thixotropic effect on the mechanical recovery characteristics of clay–structure interface. *Mar. Georesources Geotechnol.* 41, 1404–1414. doi:10.1080/1064119x.2022.2144558

Wang, Y., Zhang, S., Ren, Y., Qi, Z., and Yang, Q. (2023). Characterization of engineering properties of deep-water soils in the South China Sea. *Eng. Geol.* 320, 107138. doi:10.1016/j.enggeo.2023.107138

Wei, L., Dang, F., and Ding, J. (2023b). An investigation on the thixotropic parameters and mechanical properties of loess. *Front. Earth Sci.* 11. doi:10.3389/feart.2023.1240799

Wei, L., Dang, F., Ding, J., Wu, X., Li, J., and Cao, Z. (2023a). An analysis of thixotropic micropore variation and its mechanism in loess. *Front. Ecol. Evol.* 11. doi:10.3389/fevo.2023.1242462

Xu, J., Wu, Z., Chen, H., Shao, L., Zhou, X., and Wang, S. (2022). Influence of dry-wet cycles on the strength behavior of basalt-fiber reinforced loess. *Eng. Geol.* 302, 106645. doi:10.1016/j.enggeo.2022.106645

Xue, Y., Li, X., Liu, J., Ranjith, P. G., Gao, F., Cai, C., et al. (2024). An experimental study on mechanical properties and fracturing characteristics of granite under high-temperature heating and liquid nitrogen cooling cyclic treatment. *Geoenergy Sci. Eng.* 237, 212816. doi:10.1016/j.geoen.2024.212816

Yang, S., and Andersen, K. H. (2016). Thixotropy of marine clays. *Geotechnical Test. J.* 39, 331–339. doi:10.1520/gtj20150020

Yang, S., Ren, Y., and Andersen, K. H. (2021). Effects of thixotropy and reconsolidation on the undrained shear characteristics of remoulded marine clays. *Ocean. Eng.* 239, 109888. doi:10.1016/j.oceaneng.2021.109888

Zhang, G., Yin, H., and Degroot, D. J. (2013). Thixotropism of micron-sized saltwater clay flocs. *Géotechnique Lett.* 3, 162–165. doi:10.1680/geolett.13.00049

Zhang, X. W., Kong, L. W., Yang, A. W., and Sayem, H. M. (2017). Thixotropic mechanism of clay: a microstructural investigation. *Soils Found.* 57, 23–35. doi:10.1016/j.sandf.2017.01.002

Zhou, Z., Ma, W., Zhang, S., Mu, Y., and Li, G. (2018). Effect of freeze-thaw cycles in mechanical behaviors of frozen loess. *Cold Reg. Sci. Technol.* 146, 9–18. doi:10.1016/j.coldregions.2017.11.011

Zhou, Z., Ma, W., Zhang, S., Mu, Y., and Li, G. (2020). Experimental investigation of the path-dependent strength and deformation behaviours of frozen loess. *Eng. Geol.* 265, 105449. doi:10.1016/j.enggeo.2019.105449